


<https://doi.org/10.1038/s42003-025-07777-7>

ArgR-dependent bacterial resistance to host lipid droplets in *Edwardsiella piscicida*

Yue Peng^{1,5}, Yihan Liu^{1,5}, Junze Wu¹, Yuanxing Zhang², Qiyao Wang^{1,3,4} & Shuai Shao^{1,3,4} 

Lipid droplets (LDs), as innate immune hubs, function in the front line of antimicrobial defense involved in the host-pathogen arms race. Particularly for intracellular bacterial pathogens, the endowed capacity to resist host LDs can effectively facilitate pathogen in vivo colonization and evasion from the host's innate immune response. Here, to investigate the genetic mechanisms of intracellular bacteria response to host LDs, we utilized transposon insertion sequencing to dissect critical fitness determinants of *Edwardsiella piscicida* under the treatment of LDs isolated from its native host, turbot. Targeted metabolomics indicated that LD challenge resulted in the accumulation of intracellular arginine. The core arginine metabolism regulatory factor, ArgR, was found to play a pivotal role in combating LDs, emphasizing the importance of orchestrating intracellular arginine levels for bacterial LD adaptation. Specifically, ArgR enhanced the expressions of genes involved in arginine catabolism (*speA/B* and *arcC*) and diminished gene transcripts associated with arginine import (*artP*) and synthesis (*argD/E/H*). Furthermore, ArgR contributed to the pathogenesis of *E. piscicida*, promoting the proliferation in host cells and virulence in turbot. Collectively, our results shed light on the underlying mechanism of intracellular pathogens resisting LDs during bacterial infections and highlighting the crucial role of arginine in the host-pathogen interactions.

Lipid droplets (LDs) are phospholipid-monolayer-bound organelles found in various eukaryotic cells, primarily responsible for lipid storage and maintenance of the cellular membrane system stability¹. Despite being composed mainly of inert neutral lipids, the versatile proteins accommodated on the LDs surface endow LDs to directly participate in innate immune response². Upon infection with bacteria, viruses, or parasites, LD formation and accumulation are induced, constituting the front line in the host-pathogen arms race. For instance, viperin located on LDs exerts antiviral activity against hepatitis C virus and dengue virus³; histones on LDs facilitate *Drosophila* embryos to resist bacterial infections⁴; LDs contribute to cross-presentation of exogenous antigens^{5,6}. Especially, LDs with antibacterial activity, referred to as defensive-LDs, have been recognized as critical elements of innate immune mechanisms⁷.

LDs are vital for both pathogens and hosts involved in the dynamic process of bacterial infection⁸. For intracellular pathogens, LDs serve as a valuable nutritional and energy source to contribute to their resilience against stressful intracellular environments^{9,10}. Moreover, intracellular pathogens can manipulate LD generation

within host cells to promote their proliferation. For instance, *Salmonella* utilizes its type III secretion system (T3SS) effector, SseJ, to esterify cholesterol and increase LD production, thus stabilizing *Salmonella*-containing vacuoles and aiding in vivo survival¹¹. Furthermore, *S. Typhimurium*-induced LD formation was rapid and time-dependent with the participation of T3SS to promote bacterial replication¹². *Burkholderia pseudomallei* induced LD accumulation to interfere with macroautophagic/autophagic flux, which blocked autophagy-dependent inhibition of infection¹³.

Simultaneously, LDs also actively participate in the innate immune response to support host antimicrobial defense. Emerging evidence has revealed that LDs function as key signaling platforms where viperin recruits IRAK1 and TRAF6 to amplify the IFN-mediated immune response¹⁴. Remarkably, antimicrobial proteins would be recruited and augmented on the LD surface to directly kill intracellular pathogens. In mammalian cells, the synthesis of cationic antimicrobial peptides (CAMPs) was induced by LPS treatment, which were then loaded on LDs to inhibit the proliferation of bacterial pathogens^{15,16}.

¹State Key Laboratory of Bioreactor Engineering, East China University of Science and Technology, Shanghai, China. ²Southern Marine Science and Engineering Guangdong Laboratory (Zhuhai), 519000 Zhuhai, China. ³Shanghai Engineering Research Center of Maricultured Animal Vaccines, Shanghai, China. ⁴Laboratory of Aquatic Animal Diseases of MOA, Shanghai, China. ⁵These authors contributed equally: Yue Peng, Yihan Liu. ✉ e-mail: shaoscott@ecust.edu.cn

To succeed in escaping host immune clearance, intracellular pathogens have to evolve the ability to counteract LDs, however, the mechanisms by which pathogens directly resist antibacterial substances on LDs are not yet fully elucidated. *Edwardsiella piscicida*, a Gram-negative bacterium belonging to the Enterobacteriaceae family, can infect various commercially important aquatic species, including turbot, sea bass, and eel, posing a significant potential threat to the global aquaculture industry^{17–19}. As a typical intracellular pathogen, *E. piscicida* leverages the effectors of T3SS and type VI secretion systems (T6SS) to hijack host cells and interrupt immune response, establishing colonization within host epithelial cells and macrophages^{20,21}. Additionally, *E. piscicida* has evolved specific cell wall modification mechanisms for combating environmental stress and resisting antimicrobial substances^{22,23}. In this study, transposon insertion sequencing (Tn-seq) was employed to investigate the key fitness determinants governing the growth of *E. piscicida* upon encountering the turbot hepatic LDs. The presence of LDs resulted in the excessive accumulation of intracellular arginines, which was detrimental to bacterial resistance against the killing effects of LDs. The transcriptional regulator ArgR coordinated the expression of arginine metabolism-associated genes as well as the intracellular level of arginine, contributing to *E. piscicida*'s adaptation to host LDs. These findings highlight the pivotal role of arginine metabolism in LD-mediated host-pathogen interaction and further expand our understanding of the lifestyle of intracellular pathogens within host cells, which could be exploited as the antimicrobial strategy.

Results

Intracellular *E. piscicida* resists LD-mediated bactericidal effects

When intracellular pathogenic bacteria enter host cells through phagocytic vesicles either actively or passively, LDs armed with antimicrobial proteins can attract and directly contact the pathogenic bacteria to kill them, facilitating innate immunity¹⁵. Proteomic analysis identified several antimicrobial proteins, such as histones, on turbot liver LDs following stimulation by inactivated *E. piscicida*, supporting that LDs function as immune response organelles (Supplementary Fig. S1). To evaluate the resistance of *E. piscicida* against LDs, its growth curve was measured after the LD challenge. Hepatic LDs were extracted from turbot, which had been intraperitoneally injected with heat-inactivated bacteria as an immunity stimulus. The intracellular pathogen *Salmonella* Typhimurium SL1344, aquatic pathogen *Aeromonas veronii* GD2019, and enterohemorrhagic *Escherichia coli* O157:H7 EDL933 were used as controls. Sensitivity paper discs incubated with the purified LD suspensions were used to evaluate LD-mediated bactericidal effects. *E. piscicida*, *A. veronii*, and *Salmonella* exhibited apparent resistance against LD-mediated bactericidal effects and proliferated from 9 h post-treatment, while the growth of *E. coli* was almost completely inhibited (Fig. 1A, B). This suggested that certain pathogenic bacteria generally evolved a certain degree of resistance to LDs and antimicrobial substances on their surface to conquer host innate immune clearance. We observed that the growth inhibition caused by LDs primarily occurred during the early stages (0–12 h) and bacteria eventually overcame the LD-mediated bactericidal effects (Supplementary Fig. S3A), probably due to the nutrients, such as lipids, within the LDs promoting the secondary growth of remnant when the antimicrobial substances were depleted^{14,24}. Noteworthy, no significant difference in bactericidal activity was detected between turbot liver LDs with or without bacterial stimulation (Supplementary Fig. S2), in line with no substantial change in the abundance of antimicrobial proteins, such as histones (Supplementary Fig. S1A).

As a typical intracellular pathogen as well as the natural infectious agent of turbot, *E. piscicida* possessed the most apparent resistance to LDs among tested pathogens. The tested *E. piscicida* strains of EIB202, PPD130/90, and EIB107 all exhibited relatively stable growth after 9 h of LD challenge (Fig. 1C). The inhibition zone assays with LD-incubated discs were then conducted. A distinct antibacterial zone was observed on the agar containing *E. coli*, whereas only a minimal inhibition zone (0.9 cm) occurred on the agar containing *E. piscicida*, indicating that *E. piscicida* effectively resists LD-mediated bactericidal effects (Fig. 1D).

Tn-seq analysis of essential genes in *E. piscicida* resisting LD-mediated bactericidal effects

Adaptability to host LD-mediated bactericidal effects in pathogens may involve a series of delicate mechanisms. To this end, transposon-insertion sequencing (Tn-seq) was employed to comprehensively identify the essential genes determining the pathogen's combat LD-mediated bactericidal effects (Fig. 2A). Our previously constructed sequence-defined transposon mutant library of *E. piscicida* EIB202 was utilized for screening fitness determinants under the pressure of LDs^{25,26}. The reads per gene in the sample following growth in LD challenge condition were compared to those of the control sample grown in the normal DMEM to calculate the fold change (FC) (Fig. 2B). A total of 41 genes were identified with significant fitness differential after LD challenge ($\log_2\text{FC} > 1$ or $\log_2\text{FC} < -1$, $p < 0.05$) (Supplementary Table S1). Among them, fewer insertions were identified in 23 genes, indicating that the disruptions of these genes might impede the growth of EIB202 in the presence of LDs.

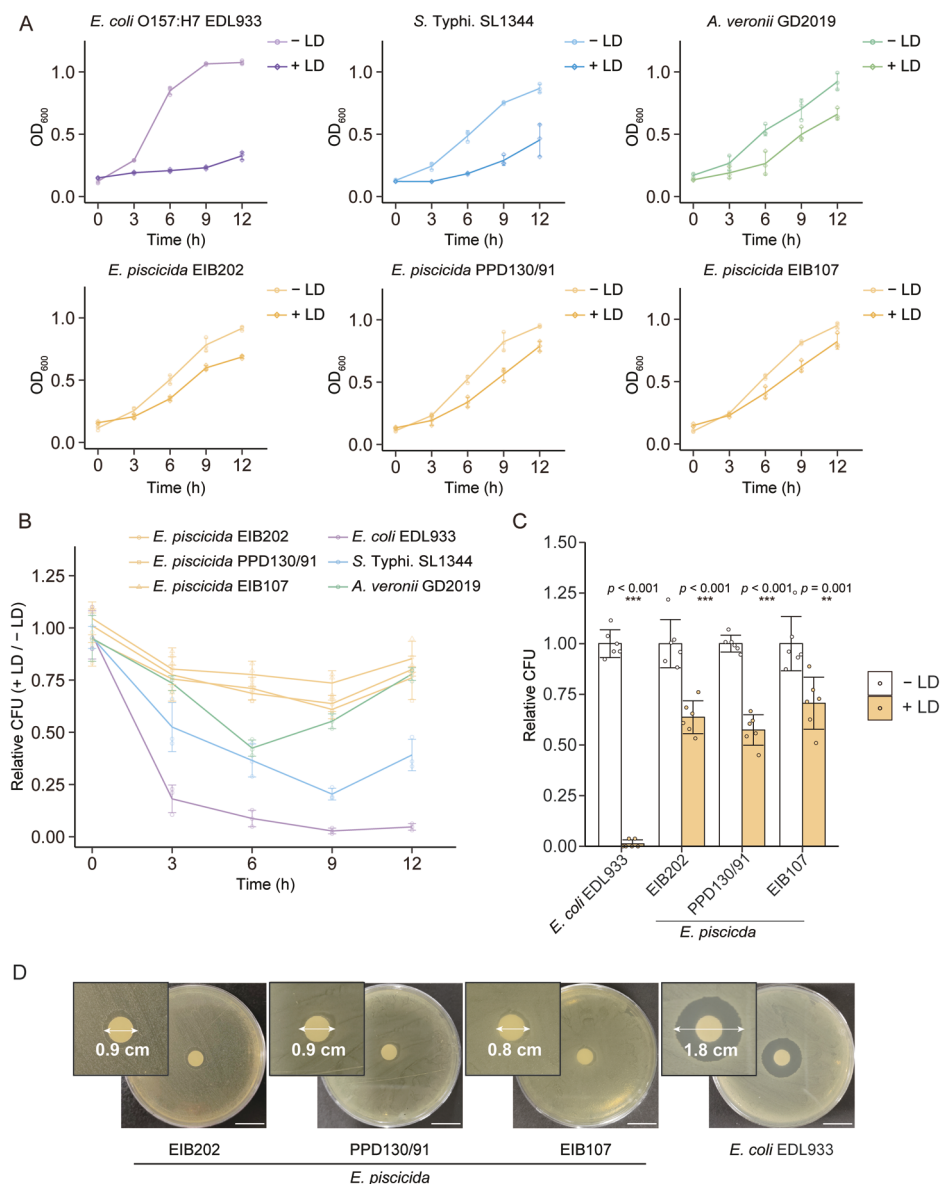
We further explored the annotated functions of these genes (Fig. 2B). Nearly half of them are involved in classical bacterial stress response and tolerance pathways, including genes associated with extracytoplasmic function sigma factors (*rpoS*, *rseB*), two-component systems (*cpxR*, *cpxP*, *qseC*), bacterial stress response (*hflC*, *hflK*, *sspB*, *rcsC*), and DNA damage repair (*recD*). Additionally, several T3SS genes (*esrB*, *escB*, *esaU*) also exhibited noticeable differences in the presence of LDs, supporting the notion that T3SS effectors participate in the interaction between pathogen and host LDs^{11,27}. Most importantly, significant fitness changes occurred in some genes related to basal metabolism, particularly those associated with specific amino acid metabolism pathways (such as *argR*), suggesting that metabolic reprogramming was undertaken to cope with LD-mediated bactericidal effects. These certain amino acid metabolic pathways may be closely connected with the LD resistance of *E. piscicida*.

Gene Ontology (GO) biological process and Kyoto Encyclopedia of Genes and Genomes (KEGG) pathway enrichment analysis were further performed to cluster the specific pathways in which the differentially expressed genes are involved (Fig. 2C, D). In the annotated functional categories, pathways related to chemotaxis, cell motility, and cell wall synthesis were enriched as well as CAMP resistance and oxidative stress response. Specifically, pathways associated with carbon metabolism, the respiratory electron transport chain, and amino acid synthesis exhibited high enrich scores, indicative of the vital role of metabolic reprogramming in response to LDs. Among them, the term “arginine biosynthesis” was enriched in both the KEGG pathway and GO biological process functional analysis. To visually explore the functional relevance among the enriched genes, the STRING database was queried to display the genes with established associations using a protein-protein interaction (PPI) network (Fig. 2E). Three interconnected clusters, including the stress response regulation and T3SS, were highlighted, of which arginine metabolism formed a distinct cluster within amino acid metabolism. These results supported the essential role of the arginine metabolism pathway in the resistance to LD-mediated bactericidal effects.

Validation of genes revealed by Tn-seq analysis for resisting LD-mediated bactericidal effects

The sequence-defined transposon library enables us to assess the impact of individual gene mutations conveniently. For the growth test in the presence of LDs, 18 insertional mutants that exhibited significant fitness differences were selected, meanwhile, four randomly selected insertional mutants (ETA_E_1610::Tn, ETA_E_2755::Tn, ETA_E_2004::Tn, ETA_E_2009::Tn) with no influences in Tn-seq analysis were used as controls (Fig. 3A). In total, 16 mutants exhibited significant differences in growth at 9 h post-LD-treatment, which was consistent with the trends observed in Tn-seq analysis and proved the reliability of our screening. Among the genes, the insertions of regulatory factors *argR*, *cpxR*, *esrB*, and *rpoS* resulted in an apparent growth reduction under the pressure of LDs, indicating their potential regulation roles in the resistance to LD-mediated bactericidal effects (Fig. 3A). The

Fig. 1 | *E. piscicida* counteracts LD-mediated bactericidal effects. **A, B** Growth profiles of different gram-negative bacteria in the presence of turbot liver LDs. *E. piscicida* and *A. veronii* were cultured in MinA minimal medium treated with LDs or PBS at 30 °C, while *S. Typhimurium* and *E. coli* were cultured at 37 °C. The value of OD₆₀₀ was measured every 3 h (**A**) and the relative CFU (**B**) was calculated by CFUs per microliter of the LD-treated group divided by CFUs per microliter of the corresponding PBS-treated group at the indicated time points ($n = 3$, 1 technical replicate per experiment). **C** CFUs of *E. piscicida* and *E. coli* cultured for 9 h in the presence of LDs or PBS ($n = 6$, 3 technical replicates per experiment). The results are shown as the mean \pm S.D. (* $P < 0.05$; ** $P < 0.01$; *** $P < 0.001$; ns not significant by Student's *t* test). **D** Inhibition zone assays of *E. piscicida* and *E. coli*. The sensitivity paper discs were incubated with purified LDs suspension with a concentration of 5 mg protein per microliter and then placed on LB plates spread with bacteria. White scale bars, 1.5 cm. The image shown is representative of three independent experiments.



multidrug efflux component *acrA* was also found to determine the resistance of *E. piscicida* to LDs.

To further investigate their impacts on the growth of *E. piscicida* responding to LD challenge, the in-frame deletion strains of indicated five genes ($\Delta argR$, $\Delta rpoS$, $\Delta esrB$, $\Delta cpxR$, $\Delta acrA$) were constructed. The growth trends of all five deletion strains were observed to exhibit noticeable growth inhibition within the first 9 h post-LD-treatment than WT did. At 9 h post-LD challenge, the difference in colony-forming units (CFU) between the deletion strains and WT reached the maximum (Fig. 3B). In line with the performance of WT, $\Delta argR$, $\Delta esrB$, and $\Delta cpxR$ possessed the growth recovery after 9 h, while the growth of $\Delta acrA$ and $\Delta rpoS$ was constantly inhibited by the same concentration of LD (Fig. 3B). Furthermore, the deletion mutants formed larger inhibition zones (1.3–1.7 cm) than WT did, while the complementary strains rescued the impaired resistance to LD-mediated bactericidal effects (Figs. 1B and 3C). These observations were congruent with results in the susceptibility assays and further validated their critical roles in the process of bacterial resistance to LDs.

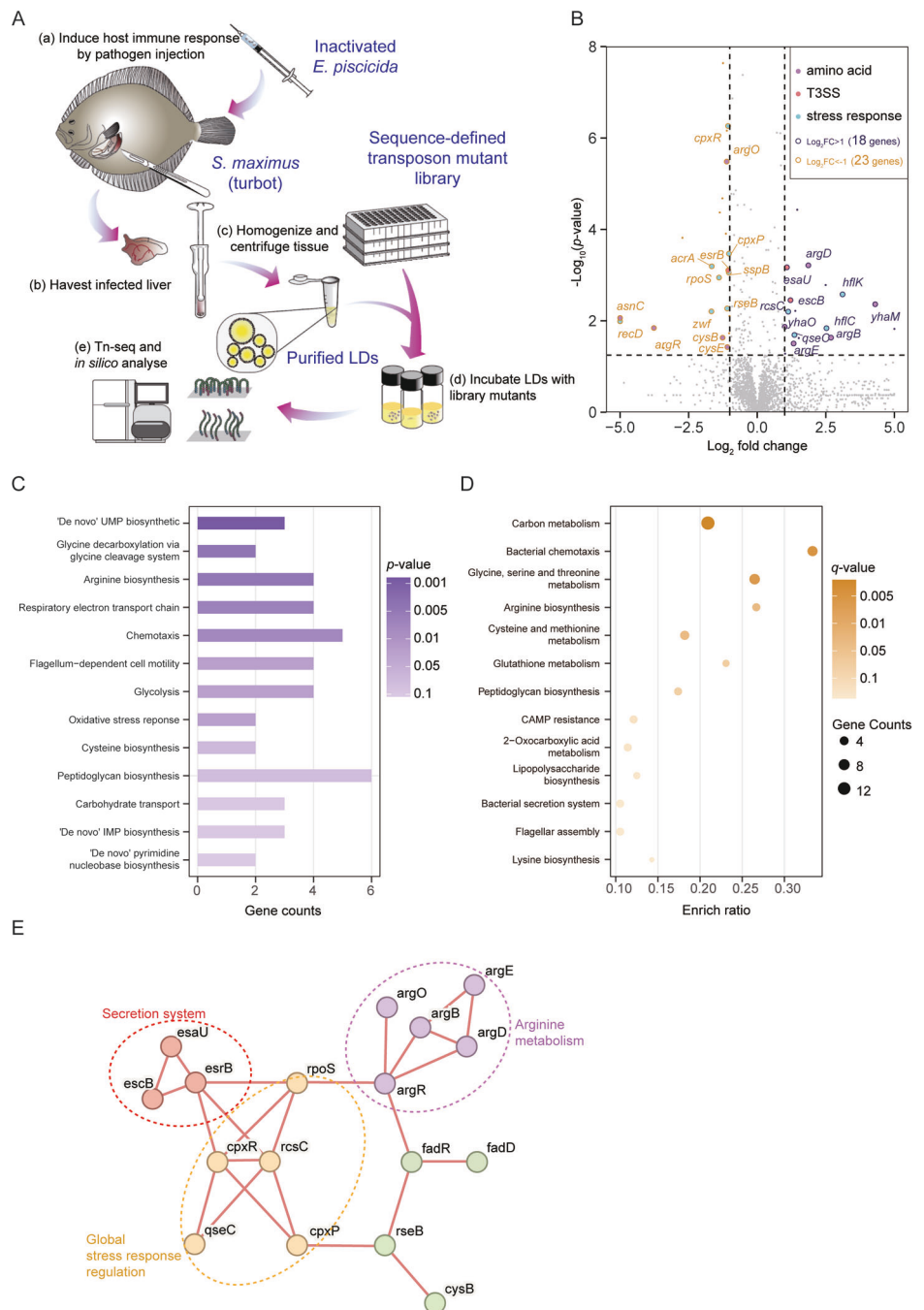
We then investigated the transcription levels of identified candidates in *E. piscicida* upon the treatment of LDs. In the presence of LDs, the

transcription level of *argR* was up-regulated by up to 4.5-fold and that of *cpxR* was enhanced to approximately 2-fold (Fig. 3D). The transcription levels of *rpoS*, *esrB*, and *acrA* exhibited no significant changes in the treatment of LDs, suggesting their contribution to LD resistance potentially at post-transcriptional levels. Considering that ArgR serves as a central regulator for arginine metabolism and is conserved in enteric pathogens (Supplementary Fig. S5), we thus supposed that arginine metabolism modulated by ArgR contributes to the resistance mechanism against LD-mediated bactericidal effects.

Arginine influences the resistance of *E. piscicida* to LD-mediated bactericidal effects in an intracellular concentration-dependent manner

Our Tn-seq data gave us the clue that genes involved in arginine metabolism may have important impacts on the growth of *E. piscicida* under LD challenge (Figs. 2B and 3A). To further analyze the correlation between arginine metabolism-related genes and their fitness changes, a gene-set enrichment analysis (GSEA) was performed from our Tn-seq data. Each gene was ranked using the normalized log₂ FC and then running enrichment scores were calculated for the defined gene sets “arginine import or synthesis” and “arginine export or catabolism” (Fig. 4A; Supplementary Table S2). The

Fig. 2 | Tn-seq analysis of essential genes in *E. piscicida* resisting LD-mediated bactericidal effects. **A** Schematic flow chart of the Tn-seq analysis. Hepatic LDs were purified from fractionated turbot liver by centrifugation in sucrose density. Each defined Tn library of *E. piscicida* EIB202 was grown in normal DMEM (control) or DMEM supplemented with LDs for 9 h at 30 °C. **B** Volcano plots illustrate the FC of the abundance of transposon insertion mutants grown in DMEM with LDs compared to those grown in normal DMEM. Genes with significantly highlighted with the cut-off of $\log_2FC > 1$ or < -1 , and $P < 0.05$. **C** GO biological process and **D** KEGG pathway enrichment analysis of highlighted genes in **B**. The enrichment ratio and counts of indicated genes in each category are shown. P -values were calculated using hypergeometric distribution and q -values representing false discovery rate were calculated by Benjamini-Hochberg procedure. **E** PPI network of genes exported from the STRING database. Each node represented the highlighted genes in **B**. Clusters were computed and manually labeled by the k-means algorithm.



running enrichment score curves for the two gene sets exhibited opposite trends: genes associated with arginine import and synthesis possessed an upward trend with positive enrichment scores, indicating that the disruptions of these genes increased *E. piscicida* fitness under LD challenge. Conversely, a downward trend with negative enrichment scores was identified among genes related to arginine degradation and export, suggesting that the interference of these genes impaired LD resistance of *E. piscicida*.

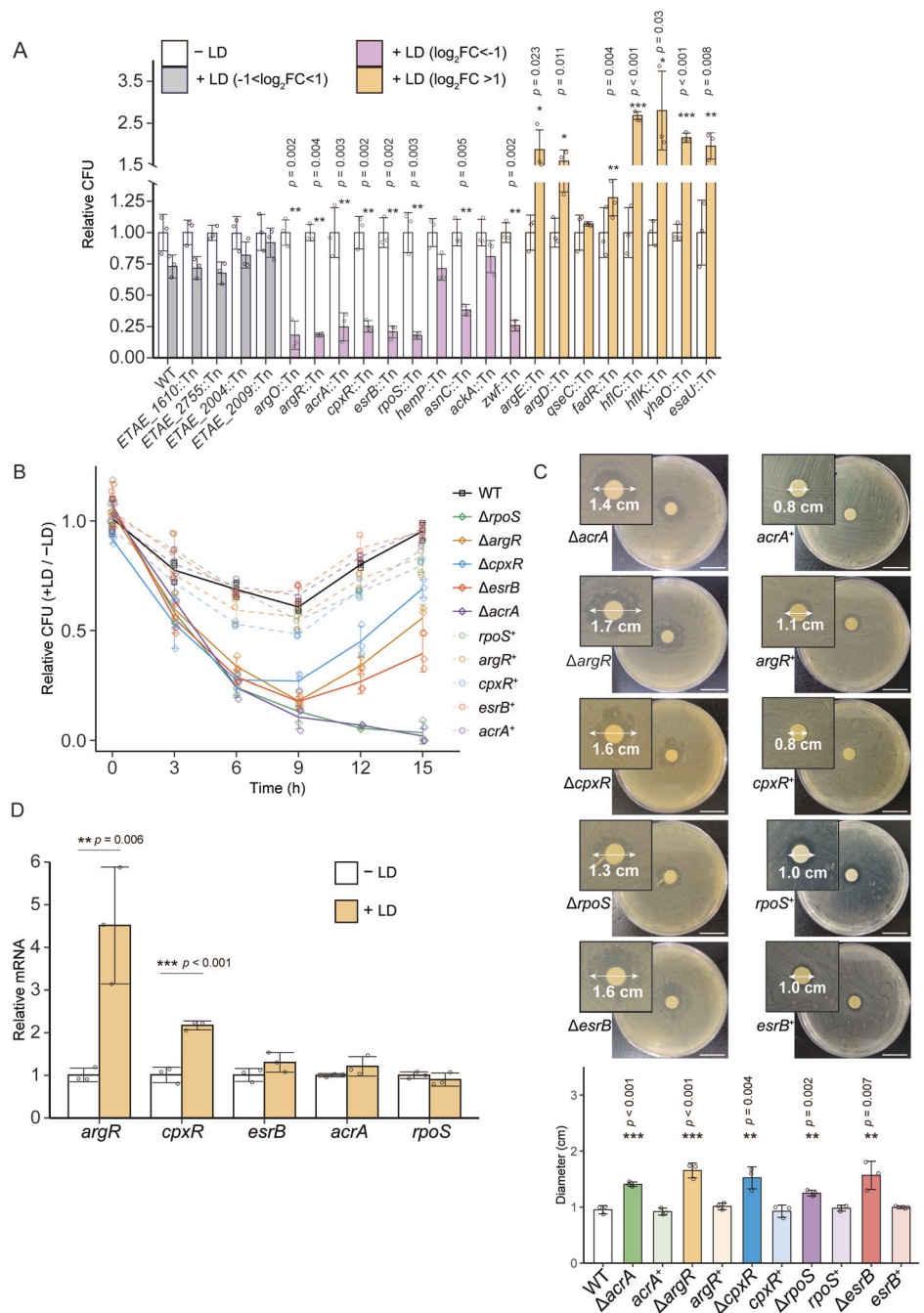
We thus hypothesized that excess intracellular arginine might interfere with the process through which *E. piscicida* combats LD-mediated bactericidal effects. To verify if intracellular arginine level is correlated with the response of *E. piscicida* against LDs, WT pellets were harvested following the incubation with LDs and the levels of amino acid metabolites were measured by targeted metabolomics (Supplementary Table S3). By a threshold of FC less than 0.5 and greater than 2, the intracellular arginine was significantly augmented compared to the control group (Fig. 4B). Given that

the majority of amino acid metabolites exhibited no abundance changes, *E. piscicida* was speculated to undergo the metabolism reprogramming of arginine under the pressure of LDs. As a repressor of arginine biosynthesis and an activator of arginine catabolism, *argR* is responsible for the balance of intracellular arginine²⁸. Considering the fine-tuning of arginine level is critical for bacteria in a stressful environment^{29,30}, this result supported the observed fitness defect of $\Delta argR$ as well as the up-regulation of *argR*.

To decipher the role of arginine metabolism in resisting LD-mediated bactericidal effects, we then focused on the performances of the genes involved in arginine metabolism (Fig. 4C). Initially, eight insertional mutants related to arginine biosynthesis from glutamate (*argD*::Tn, *argH*::Tn, *argE*::Tn), arginine deiminase pathway (*arcC*::Tn), arginine decarboxylation (*speA*::Tn, *speB*::Tn) along with arginine exportation (*argO*::Tn), and importation (*artP*::Tn) were selected and their growth was tested in the presence of LDs. The insertion in arginine exporter *argO*

Fig. 3 | Validation of critical genes revealed by Tn-seq analysis for resisting LD-mediated killing effects.

A CFUs of WT *E. piscicida* and indicated transposon insertion mutants grown in MinA medium with LDs or PBS at 30 °C for 9 h. The corresponding insertion mutants were picked from the defined Tn-library according to our Tn-seq results, including genes with more insertions ($\log_2FC > 1$, purple), genes with fewer insertions ($\log_2FC < -1$, yellow), and not significantly changed genes ($0.5 < FC < 2$, black) ($n = 3$, 3 technical replicates per experiment). **B** Normalized growth curve of *E. piscicida* variants in the presence of LDs. WT, $\Delta rpoS$, $\Delta argR$, $\Delta cpxR$, $\Delta esrB$, $\Delta acrA$ and five corresponding complementary strains were grown in MinA medium supplemented with LDs at 30 °C for 12 h. The relative CFU of each strain was normalized to corresponding CFUs per microliter in MinA medium with PBS (control). ($n = 3$, 3 technical replicates per experiment). **C** Inhibition zone assays of *E. piscicida* variants in the presence of paper discs containing LD suspension. Bar plot represents the measured diameters of the indicated deletion mutants and their complementary strains (cpl) as well as *E. piscicida* WT ($n = 3$, 1 technical replicate per experiment). White scale bars, 1.5 cm. The disc size, 0.6 cm. The image shown is representative of at least three independent experiments. **D** The relative transcripts of *argR* and *cpxR* in *E. piscicida* WT in the presence and absence of LDs for 9 h. *gyrB* was used as a negative control ($n = 3$, 3 technical replicates per experiment). The results are shown as the mean \pm S.D. (* $P < 0.05$; ** $P < 0.01$; *** $P < 0.001$; ns not significant by Student's *t* test).



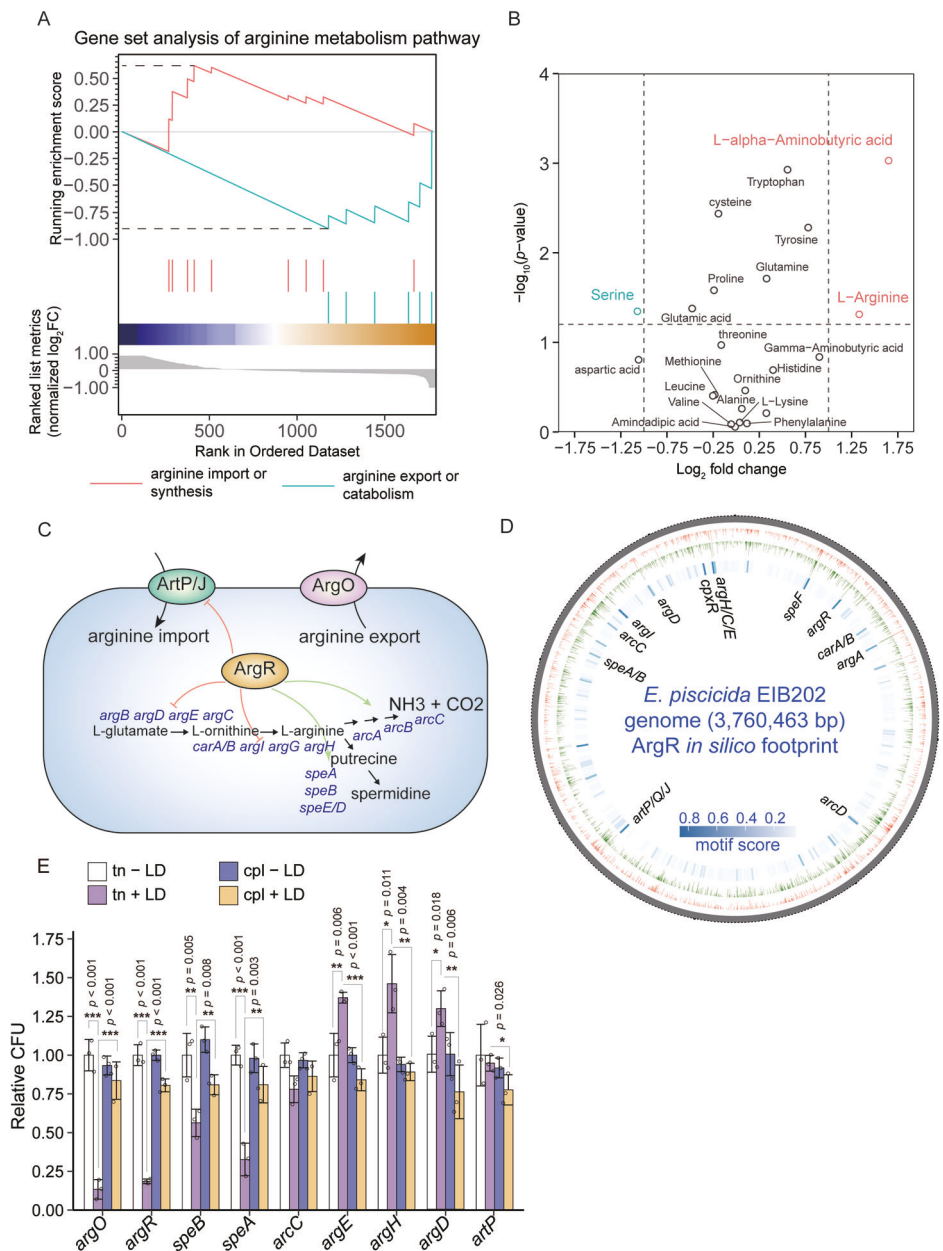
impaired the resistance of *E. piscicida* to LDs, whereas the blockage of the arginine generation (*argD*, *argE*, and *argH*) enhanced the viability under the pressure of LDs, indicating the importance of the appropriate level of intracellular arginine (Fig. 4D). Similarly, the insertional mutations of *speA* and *speB*, involved in converting arginine to putrescine/spermidine, resulted in weakened growth after LD challenge (Fig. 4D). However, the mutation of *arcC*, which converts arginine to ornithine, had no significant influence on the resistance to LDs. Additionally, we successfully obtained the corresponding deletion mutants except for *speA/argE* and they exhibited similar tendency against LD-mediated bactericidal effects (Supplementary Fig. S3B). These findings suggested that the elimination of the excessive intracellular arginine is vital for the LD resistance of *E. piscicida*.

To further investigate the role of ArgR involved in arginine metabolism under LD challenge, we initially utilized the conserved ArgR binding motif (previously characterized in *E. coli*) to scan the *E. piscicida*

genome (Fig. 4E). The in silico DNA footprint analysis indicated that ArgR potentially binds to the promoter regions of genes involved in arginine metabolism, including *argE/H/D*, *speA/B*, *arcC*, and *artP*. (Supplementary Table S4). Electrophoretic mobility shift assay (EMSA) was further conducted and confirmed the binding ability of ArgR to the promoters of *speA/B*, *argE/H*, *argD*, and *artP* (Supplementary Fig. S4). We then compared the transcription levels of arginine metabolism-related genes in WT and $\Delta argR$ under LD challenge (Fig. 5A). In congruent with increased intracellular arginine levels observed in metabolomics, LD challenge significantly enhanced the transcription levels of tested genes in WT, reflecting the activation of arginine metabolism. The absence of *argR* resulted in the down-regulations of *speA/B* and *arcC* and the up-regulations of *argE/H/D* and *artP*, indicating the role of ArgR in repressing arginine import or synthesis and activating arginine export or catabolism (Fig. 4C). The presence of *argR* had no influences on *argO*

Fig. 4 | Genes involved in arginine metabolism contribute to resisting LD-mediated killing effects.

A GSEA of genes involved in arginine import or synthesis (red) and export or catabolism (light blue). Background genes were chosen from Tn-seq analysis and genes without any reads were excluded. The ranked list metric represents normalized \log_2FC in Tn-seq and the running score was calculated by R package clusterprofiler. **B** Volcano plot illustrating the abundance changes of amino acid-related metabolites in *E. piscicida* grown in LD-treated MinA minimal medium compared to those grown in PBS-treated medium. A total of 22 amino acid-related metabolites were quantified by targeted metabolomics using UPLC-MS/MS. Metabolites with significantly highlighted by the cut-off of $\log_2FC > 1$ or < -1 , and $p < 0.05$. **C** Schematic of bacterial arginine metabolism and the regulation of ArgR. **D** CFUs of WT *E. piscicida* and arginine metabolism-related transposon insertion mutants (tn) and corresponding complementary strains (cpl) in the presence and absence of LDs at 30 °C for 9 h. The complementary strains were constructed via pUTt vectors carrying the complemented genes. The results are shown as the mean \pm S.D. ($n = 3$, 3 technical replicates per experiment, $*P < 0.05$; $**P < 0.01$; $***P < 0.001$; ns not significant by Student's t test). **E** Circos plot of in silico footprint assay result of ArgR. Experimental validated ArgR binding motif 1 (red track) and ArgR binding motif 2 (green track) in *E. coli* were used for predicting the ArgR binding sites across *E. piscicida* EIB202 genome. Motif scores (blue track) were calculated by the average of two binding motif scores. The motif scores were computed with FIMO software and genes related to arginine metabolism were highlighted in the inner track. A motif score cutoff of 0.5 was applied to highlight significant results.



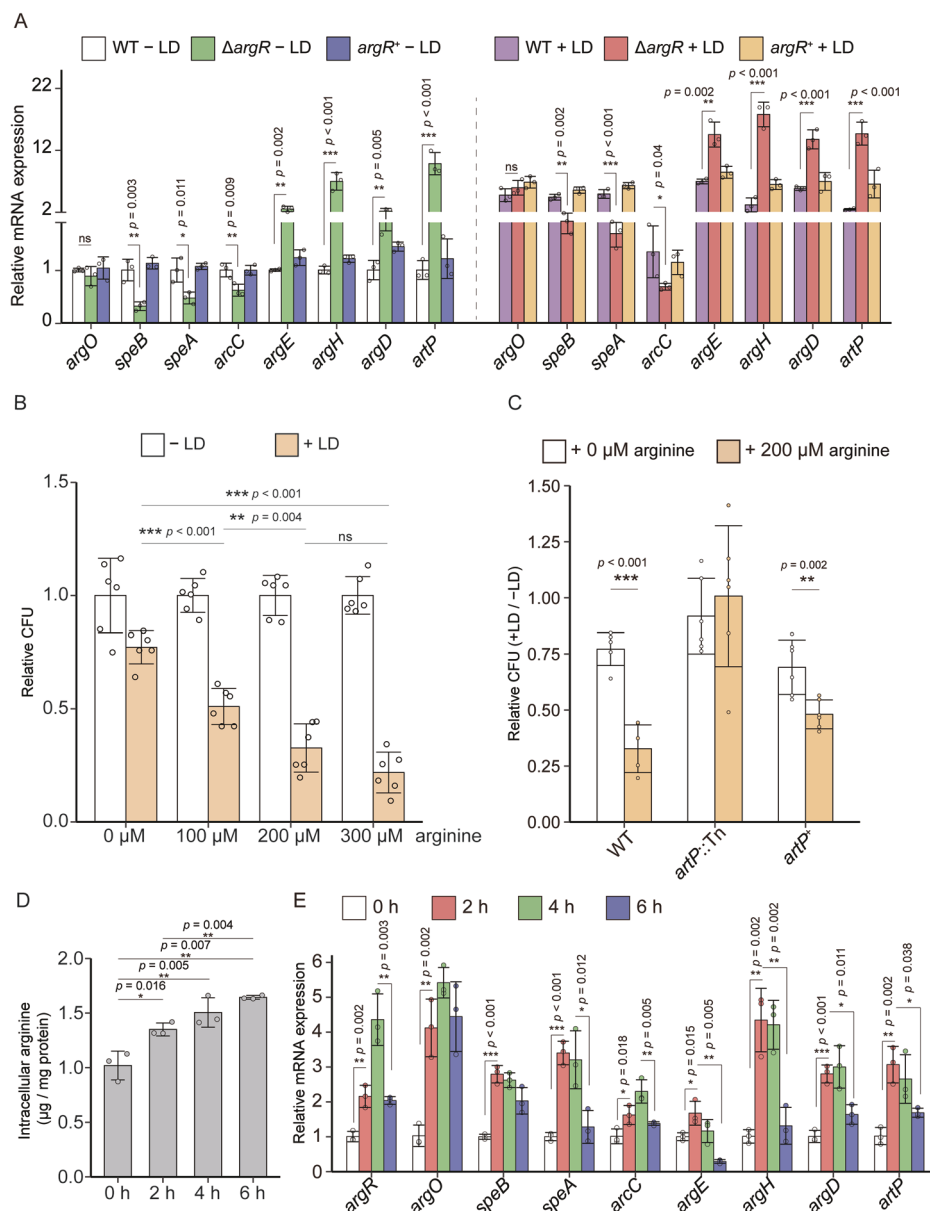
transcripts, aligning with no predicted ArgR-binding sites in *argO*'s promoter region. More importantly, LD challenge amplified the activation of *argE/D/H* and *artP* and the repression of *speA/B* caused by the absence of *argR*. Collectively, it can be concluded that LD challenge stimulates intracellular arginine accumulation and *argR* is responsible for the maintenance of arginine homeostasis, conferring LD resistance on *E. piscicida*.

Given that the intracellular arginine directly participates in bacterial pH regulation, biofilm formation, and resistance to antimicrobial substances^{30–32}, we further aimed to investigate the direct impact of arginine on the LD resistance of *E. piscicida*. To this end, a gradient concentration of 0, 100, 200, and 300 μ M arginine was added into the medium and the growth of *E. piscicida* was assessed in the presence and absence of LDs, respectively. All the gradient arginine concentrations did not influence the growth of WT without LD challenge (Fig. 5B). In the presence of LDs, the growth of WT gradually slowed down with the increased concentration of arginine, suggesting excessive arginine attenuated the LD resistance of *E. piscicida* (Fig. 5B). Furthermore, when the extracellular arginine transport

gene *artP* was mutated, the addition of arginine no longer had a significant impact on the LD resistance of *E. piscicida* (Fig. 5C). The complement of *artP* restored the weakened LD resistance as WT did (Fig. 5C). These results proved that excessive intracellular arginine impairs the LD resistance of *E. piscicida*.

To investigate the intracellular arginine levels within host cells during *E. piscicida* infection, enzyme-linked immunosorbent assay (ELISA) was performed and indicated that intracellular arginine levels in RAW264.7 gradually accumulated throughout infection, suggesting that arginine may participate in the LD-mediated defense mechanisms (Fig. 5D). To cope with the augmented arginine within host cells, qRT-PCR analysis further revealed the altered expression of *argR* and other arginine metabolism-related genes in *E. piscicida* throughout the infection (Fig. 5E). During the early phase of the infection (0–2 h), all arginine metabolism-related genes were upregulated in *E. piscicida*, consistent with the stimulated arginine metabolism in response to LD challenge. At 6 h post-infection, the expression of *argD/E/H* and *artP* was significantly reduced, while the transcripts of *argO* and *speB* remained at relatively high levels. It might be

Fig. 5 | Arginine attenuates *E. piscicida*'s resistance to LD-mediated killing effects in an intracellular concentration-dependent manner. **A** The relative transcripts of arginine metabolism-related genes in WT, $\Delta argR$, and $argR^+$ grown in MinA medium with LDs or PBS for 9 h. *gyrB* was used as a negative control ($n = 3$, 3 technical replicates per experiment). **B** CFUs of WT *E. piscicida* grown in MinA medium with LDs or PBS at 30 °C for 9 h and supplemented with different concentrations of arginine ($n = 6$, 3 technical replicates per experiment). **C** CFUs of *E. piscicida* transposon insertion mutant *artP::Tn* and the complementary strains *artP⁺* grown in MinA medium with LDs or PBS in the presence and absence of 200 μ M arginine ($n = 6$, 3 technical replicates per experiment). **D, E** Intracellular arginine levels and relative transcription levels of arginine metabolism-related genes throughout infection. RAW264.7 cells were infected with *E. piscicida* (WT) at an MOI of 10, and then cells were lysed before centrifuged to collect intracellular bacteria. *gyrB* was used as a negative control ($n = 3$, 2 technical replicates per experiment) (**D**). Intracellular bacteria were collected for qRT-PCR analysis. *gyrB* was used as a negative control ($n = 3$, 3 technical replicates per experiment) (**E**). The results are shown as the mean \pm S.D. * $P < 0.05$; ** $P < 0.01$; *** $P < 0.001$; ns not significant by Student's *t* test.



explained by the fact that *E. piscicida* attenuates de novo arginine synthesis/import and promotes arginine degradation/export to maintain arginine homeostasis and achieve immune evasion.

argR determines the ex vivo and in vivo pathogenesis of *E. piscicida*

To investigate the impact of LD resistance essential genes on the pathogenesis of *E. piscicida*, arginine metabolism-related mutants ($\Delta argR$, $\Delta argO$, $\Delta speB$), as well as global stress tolerance-related mutants ($\Delta acrA$ and $\Delta cpxR$), were employed to infect RAW264.7 cells at a multiplicity of infection (MOI) of 10. Given that *esrB* and *rpoS* have been previously validated as critical virulence determinants of *E. piscicida*^{33,34}, they were not included. Similar to the pathogenicity attenuated strain $\Delta T3SS$ losing T3SS function, CFU counts of $\Delta argR$, $\Delta argO$, $\Delta speB$, $\Delta acrA$, and $\Delta cpxR$ significantly decreased inside macrophages compared to that of WT while the corresponding complementary strains restored the intracellular CFUs, reflecting their reduced colonization and proliferation in host cells (Fig. 6A).

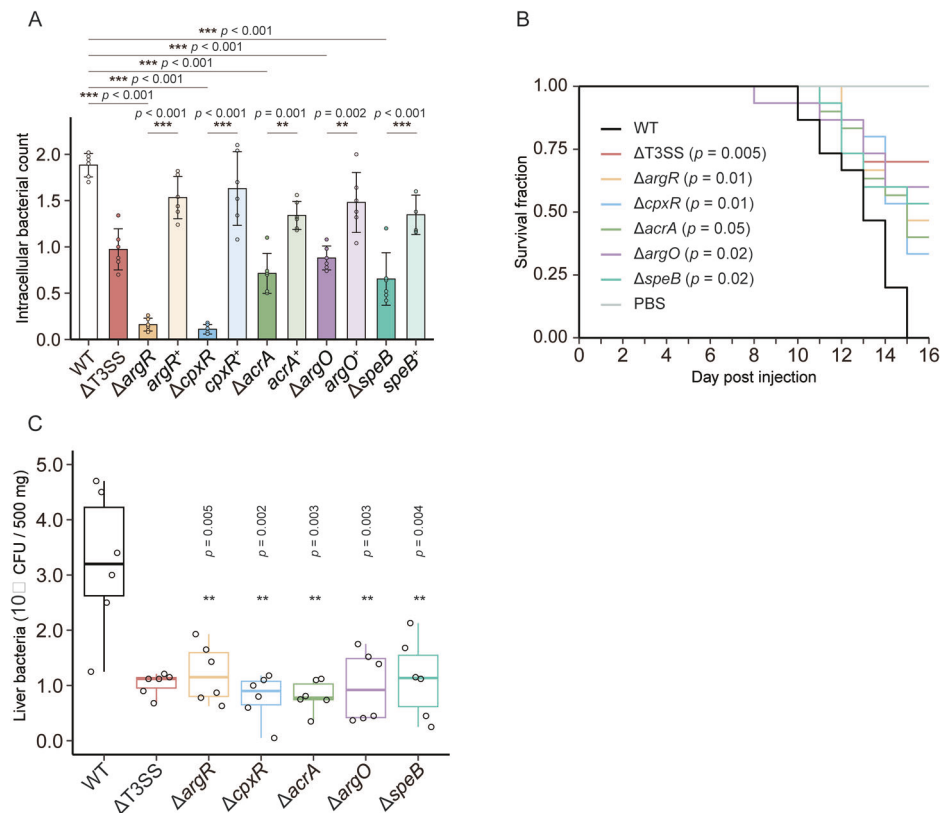
To determine the role of *argR*, *argO*, *speB*, *acrA*, and *cpxR* during the in vivo invasion process, the mutants were intraperitoneally injected into turbot at a dose of 5×10^6 CFU/fish, and then the survival curve was plotted

(Fig. 6B). From the curve, turbot infected with WT began to show signs of mortality at 10 days post-injection (dpi) and were with complete mortality by 14 dpi. In contrast, turbot from $\Delta argR$, $\Delta argO$, $\Delta speB$, $\Delta acrA$, and $\Delta cpxR$ infected groups exhibited a delayed onset of mortality as well as higher survival rates (Fig. 6B). Subsequently, liver tissue was collected at 10 dpi and the colonization was counted by spreading the hepatic homogenate on deoxycholate hydrogen sulfide lactose (DHL) agar. Bacterial load of $\Delta argR$, $\Delta argO$, $\Delta speB$, $\Delta acrA$, and $\Delta cpxR$ were observed with a significant reduction in the liver (Fig. 6C). These findings demonstrated that *argR*, *argO*, *speB*, *acrA*, and *cpxR* function as virulence determinants in the pathogenesis of *E. piscicida*.

Discussion

Substantial evidence from previous studies has indicated the vital role of LDs in the interactions between eukaryotic host cells and pathogens. LDs serve as the potential nutrition and energy source for intracellular pathogens' colonization and proliferation, in one respect, however, various antimicrobial proteins accommodated on LDs highlight the immune defense mediated by LDs^{4,15}. In this study, we utilized Tn-seq to identify critical fitness determinants of *E. piscicida* counteracting LD-mediated bactericidal

Fig. 6 | ArgR determines the ex vivo and in vivo pathogenesis of *E. piscicida*. **A** Intracellular replication ability of *E. piscicida* variants. RAW264.7 cells were infected at an MOI of 10. The CFU of intracellular *E. piscicida* variants at 6 h post-infection was normalized to cell numbers to determine the bacterial proliferation capacity ($n = 6$, 3 technical replicates per experiment). **B** Survival curve of turbot infected with *E. piscicida* variants. A total of 15 turbot per group were used. The significance was determined by the Log-rank test by running the survival R package. **C** CFUs recovered from liver samples of turbot with infected *E. piscicida* variants. Livers were harvested at 14 days post-injection and CFUs were counted according to the colonies on DHL plates. The central line within each box represents the median, while the box represents the interquartile range (IQR), and the whiskers extend to 1.5 times the IQR ($n = 6$, 3 technical replicates per experiment). (* $P < 0.05$; ** $P < 0.01$; *** $P < 0.001$; ns not significant by Student's *t* test).



effects. The presence of LDs resulted in the accumulation of intracellular arginine. The maintenance of intracellular arginine homeostasis by ArgR-regulated arginine metabolism-associated genes was vital for *E. piscicida*'s adaptation to host LDs. Furthermore, ArgR promoted the pathogenesis of *E. piscicida*, including the proliferation in cells and virulence in turbot.

Similar to LDs in mammalian cells, hepatic LDs isolated from turbot exhibited antimicrobial effects on numerous gram-negative bacteria. The proteome analysis indicated that turbot liver LDs are abundant with histones that exhibit antimicrobial activities¹⁶. Recent findings also proved that under the stimulation of bacterial pathogens, CAMPs were specifically recruited to LDs to enhance antimicrobial capacity². These two kinds of protein can inhibit bacterial growth by polarization of bacterial membrane and disruption of membrane integrity as well as proton gradient. *E. piscicida* encodes multiple sets of cell wall modification genes, which might partly explain the enhanced resistance to LDs^{22,23}. However, although a conserved CAMP-resistance mechanism has also been identified in *Salmonella*²³, *S. Typhimurium* SL1344 displayed weaker resistance to LDs compared to *E. piscicida* EIB202. What is more, *Pseudomonas plecoglossicida*, lacking such genes, also counteracted LD-mediated bactericidal effects. These results suggested that different bacteria employ diverse and intricate mechanisms upon encountering LDs, which are not solely limited to resist histones or CAMPs.

As a result of the co-evolution with the host immune system, intracellular pathogens are urged to evolve strategies to resist LD-mediated bactericidal effects. From our Tn-seq results, *E. piscicida* employed several global regulators, including EsrB, CpxR, RpoS, and ArgR along with a multi-drug efflux complex component AcrA to cope with LD-mediated bactericidal effects. Of them, CpxR is responsible for envelope stress response and AcrA participates in the efflux of antibiotic substrates which are supposed to assist *E. piscicida* in resisting toxic substrates like CAMP or histones located on LDs^{35,36}. Our previous RNA-seq data of *E. piscicida* indicated that regulatory factors EsrB and RpoS govern a bunch of genes involved in arginine metabolism and transportation which is crucial for bacterial stress response and virulence^{33,34}.

Moreover, our Tn-seq analysis also discovered that T3SS proteins influenced the LD resistance of *E. piscicida*, which are mainly regulated by EsrB and RpoS³³. These findings highlighted the potential intersecting transcription networks that govern LD resistance of *E. piscicida*.

Arginine, as a crucial metabolite as well as a signaling molecule, has been validated to play a significant regulatory role in the interaction between pathogens and host immune response. During infection, arginine has been shown to mediate the metabolic reprogramming of cells and enhance host defense against bacterial pathogens as the sole substrate for the synthesis of nitric oxide (NO) by inducible nitric oxide synthase (iNOS)³⁷. Alternatively, the conversion of arginine into ornithine catalyzed by Arg1 has been considered as the hallmark of M2-polarized macrophages³⁸. On the other hand, arginine is also a key metabolite affecting bacterial stress tolerance and virulence^{31,39}. Arginine can serve as a buffering substance to help *S. Typhimurium* survive in extremely acidic environments and affect biofilm formation to alter antibiotic resistance in *Staphylococcus aureus*^{30,31}. Arginine derivatives, such as spermine and putrescine, prevent intracellular pathogens from clearance within macrophages⁴⁰. During infection, ArgR of enterohemorrhagic *E. coli* sensed arginine fluctuations to directly regulate the expression of T3SS genes and *E. piscicida* reprogrammed its arginine metabolism to evade NLRP3 inflammasome^{39,41}.

In conclusion, these findings contribute to revealing the pivotal role of arginine metabolism as a key determinant during the interaction between bacterial pathogens and host. Once entered into host cells, arginine in *E. piscicida* would be significantly augmented in response to LDs, and thus, *E. piscicida* has to undergo metabolic reprogramming to survive and achieve immune evasion. To cope with LD-mediated bactericidal effects, ArgR governs bacterial arginine homeostasis, by enhancing the expressions of genes involved in arginine catabolism (*speA/B* and *arcC*) and diminishing gene transcripts associated with arginine import (*artP*) and synthesis (*argD/E/H*). Nevertheless, our in vitro LD challenge assay primarily reflects the direct antimicrobial capacity of LDs. Besides, the isolated LDs contain few residual cytosolic fraction following centrifugation-extraction, such as proteins, amino acids, and sugars, which might participate in LD-mediated

bactericidal effects. Therefore, future studies should focus more on the comprehensive LD-mediated innate immunity within host.

Methods

Bacterial strains and culture conditions

The wild-type (WT) *E. piscicida* strain EIB202 (CCTCC M208068) was isolated from a diseased turbot in Yantai, China. Details of all bacterial strains and plasmids utilized in this study are presented in Supplementary Table S5. The primers applied in this study are listed in Supplementary Table S6. All *E. piscicida* strains were inoculated into lysogeny broth (LB) medium at 30 °C overnight and then were sub-cultured into a secondary medium at a dilution rate of 1:100. In LD-resistance assays, bacteria were sub-cultured in MinA minimal medium⁴² supplemented with 10 µM MgSO₄ and 0.25% casamino acids. For bacterial growth, *E. coli* O157:H7 EDL933 and *S. Typhimurium* SL1344 were cultured at 37 °C. *A. veronii* GD2019 and *P. pleuroglossicida* were grown at 30 °C. Antibiotics were added with the following concentrations when necessary: ampicillin (Amp, Sangon Biotech, A429319, 100 µg/ml), polymyxin (Col, Sangon Biotech, A610318, 30 µg/ml), kanamycin (Km, Sangon Biotech, 60206ES, 100 µg/ml), and gentamicin (Gm, Sangon Biotech, A428430, 20 µg/ml).

Turbot hepatic LD purification

The hepatic LDs were extracted and purified using a tissue homogenization sucrose gradient centrifugation method¹⁵. The liver harvested from turbot was perfused with pre-cold phosphate-buffered saline (PBS) buffer and washed twice. After being chopped into pieces smaller than 1 cm³ in volume, the liver tissues were transferred into the Dounce tissue grinder with LD purification buffer A (25% (w/v) sucrose, pH 7.5, 10 mM HEPES) at a ratio of 1 g of tissue to 1 ml of buffer and homogenized on ice. The homogenate was then aliquoted into 2 ml Eppendorf (EP) tubes and centrifuged at 15,000 × g for 90 min at 4 °C to separate different cellular components. The top fraction containing floated LDs was collected and transferred to 1.5 ml EP tubes for purification. The LD purification buffer B (100 mM KCl, pH 7.5, 25 mM Tris-HCl) was added on top of the LD fractions at a volume ratio of 1:1 and the fractions were then centrifuged at 4000 × g for 5 min at 4 °C. The bottom fraction was carefully removed using a 23 G syringe followed by adding the same volume of buffer B. This step was repeated 2 or 3 times until the lower liquid fraction was completely transparent. Purified LD samples were then resuspended in sterile PBS and stored at −20 °C for subsequent experiments. To quantify LDs, a BCA protein assay kit (Sangon, C503021) was used to determine the concentration of lipid-protein. For quality control (QC) of each LD extraction batch, western blot was performed to detect the levels of the LD protein marker (PLIN2) and β-actin in both the LD and post-centrifugation cytosolic (CYTO) fractions. Customized antibody of PLIN2 was generated by Genscript. Rabbit polyclonal anti-β-actin (ABclonal, WH400517) and corresponding secondary antibody (YEA-SEN, 34850ES60) were used. All the antibodies were diluted at a ratio of 1:1000.

LD protein samples were prepared using acetone precipitation method¹⁵. The LD fraction suspension was mixed with four volumes of ice-cold acetone and incubated at −20 °C for 24 h. After precipitation, the sample was centrifuged at 15,000 × g for 10 min at 4 °C, and the supernatant was discarded. The pellet was washed 2–3 times with ice-cold acetone and then resuspended in 10 mM Tris-HCl with 5% SDS. After sonication, the sample was warmed at 50 °C for at least 10 min. Protein samples were quantified using the BCA assay and subjected to 4D label-free quantitative proteomics.

LD challenge assays

Due to the physical nature of lipids, LDs can hardly be dissolved in the aqueous phase evenly and tend to float above. To overcome this problem, the drug sensitivity testing disc was used as the carrier of LDs in the medium. The sensitive disc-assay method for LDs was performed⁴. Generally, the protein concentration of purified LD suspension was quantified and then diluted by PBS to the protein concentration of 5 mg/ml in a 1.5 ml EP tube.

Blank sensitivity discs were immersed in LD suspension and incubated for 1 h at 4 °C on a rotating mixer. Subsequently, discs that fully absorbed LDs were placed on a clean sterile plate to evaporate excess moisture for 30 min at 4 °C.

For LD challenge assays in liquid cultures, discs loaded with LDs were immersed in the medium at a dose of 1 disc per 500 ml medium and incubated for 30 min. For control groups, discs incubated with sterile PBS were used. After the ingredients of LDs were fully released into the medium, the discs were removed and bacterial cultures grown to an optical density of OD₆₀₀ = 1 were diluted 1:100 into the MinA medium pretreated with LD- or PBS-loaded discs. Cultures were grown at 30 °C in a shaking incubator. Serial dilutions made in PBS were plated in triplicate on LB agar plates and CFUs per microliter were quantified after incubating at 30 °C overnight. The relative CFU was calculated by dividing by the CFUs per microliter of the corresponding PBS discs treated group.

For determining the inhibition zone of LDs, sensitivity discs (size of 0.6 cm in diameter) were prepared as the same procedure mentioned above. Overnight cultures grown to OD₆₀₀ = 1 were diluted 1:100 in sterile PBS. After spreading the dilutions on 7 cm LB agar plates, the discs were placed and the static incubation was performed at 30 °C overnight before measuring the diameter of the inhibition zone around the discs.

Growth profiles

Growth curve experiments were performed using sterile, clear bottom, black 96-well microplates. Overnight cultures grown to OD₆₀₀ = 1 in LB medium were diluted 1:100 into MinA medium supplemented with LDs. The bacterial solution was aliquoted to 200 µl for each well. For OD₆₀₀ measurement experiments, The Infinite® F50 multi-mode plate reader (Bioscreen) was used to monitor bacterial growth. The temperature setpoint was 30 °C and preheated before measurements. Growth curves were measured every 1 h for up to 21 h. For CFU measurement, bacterial solution in each well of the microplate was sampled every 3 h after the incubation began. Serial dilutions were made in PBS and plated on LB agar for each sample. The normalized growth curve was constructed by calculating the relative CFU at every time point.

LD resistance screening by Tn-seq analysis

The saturated transposon insertion mutant library was initially inoculated into LB medium at 30 °C and agitated for 2 h until the OD₆₀₀ reached 1.0^{25,26}. Subsequently, bacterial cultures were centrifuged at 8000 × g for 2 min, washed twice with PBS, and diluted 1:100 into DMEM (Sangon Biotech, E600003) treated with discs pre-incubated in LD suspension with 5 mg/ml protein concentration (LD group) and PBS (Control group), respectively. After shaking for 9 h, bacteria were pelleted, plated on LB agar plates, and then cultured overnight at 30 °C to eliminate DNA contamination from dead cells before genomic DNA extraction.

Tn-seq experiments procedures and data analysis were conducted⁴³. Briefly, the fragmented genomic DNAs were subjected to end repairing, A-tailing, adapters, and P5/P7 primers, generating high-throughput sequencing libraries for sequencing on the Illumina MiSeq platform. The raw sequencing data was processed by Bowtie algorithm to generate sequences mapped to *E. piscicida* EIB202 genome and Transit software was employed to process locus tallying for each locus of EIB202^{44,45}. The sum of read counts of all locus within a gene represents the read counts of this gene and the FC of each gene was computed by the LD group read counts divided by the corresponding control group read counts after normalization.

Construction of deletion and complementary strains

The in-frame deletion mutants of the indicated genes were constructed using the *sacB*-based allelic exchange method⁴⁶. Briefly, the suicide vectors pDM4, which contained the upstream and downstream sequences required for in-frame deletions of each gene (Supplementary Table S5), were transformed into *E. coli* SM10 strain and then conjugated with *E. piscicida* EIB202. After the double-crossover recombination process, the deletion mutants were then selected on LB plates containing 12% sucrose and

confirmed by PCR. For the construction of complementary strain, the pUTat vectors cloned with the intact gene sequence were generated followed by the transformation via electroporation into the corresponding deletion mutants (Supplementary Table S5).

Total RNA extraction and qRT-PCR

Total RNA samples were extracted from *E. piscicida* that were grown in MinA medium for 9 h supplemented with LDs and PBS, using an RNA isolation kit (BioFlux, BSC52S1). The mRNAs were immediately reverse-transcribed into cDNAs using a FastKing RT kit (Tiangen, KR11601). The qRT-PCR experiments were performed on an Applied Biosystems 7500 real-time system (Applied Biosystems, CA). Comparative CT method was further used to determine the relative quantities of each transcript, normalized to the *gyrB* gene which serves as a control. All primers used for qRT-PCR are listed in Supplementary Table S6.

Targeted metabolomics of intracellular amino acid metabolites

Bacteria grown in MinA medium supplemented with LDs and PBS for 9 h were harvested by centrifugation at $8000 \times g$ at 4 °C. After washed twice with pre-cold PBS, the pellet samples of each group were stored in EP tubes at −80 °C. CFU of each sample was quantified by serial dilution and plating on LB agar. The quantified samples were thawed on ice and added with 120 µl of methanol solution containing internal standards. The samples were then subjected to ultrasonic disruption at 4 °C and centrifuged at $18,000 \times g$ for 15 min. Subsequently, 10 µl of the supernatant was mixed with 70 µl of borate buffer (1/4, pH = 8.8) and 20 µl of 6-aminoquinolyl-N-hydroxysuccinimidyl carbamate (AQC) derivatization reagent (1.5 mg/ml) followed by incubation for 10 min at 55 °C. After that, a 100 µl aliquot was taken, mixed with 900 µl of ultrapure water, and then subjected to UPLC-MS/MS analysis.

DNA-binding analysis of ArgR

To determine the potential binding sites of transcription factor ArgR on the genome of *E. piscicida* EIB202, previously validated ArgR DNA-binding motif in *E. coli*, ARG Box1 (MX000116 in PRODORIC database) and ARG Box2^{47,48}, were used to predict the potential ArgR DNA-binding sites in *E. piscicida*. Binding motifs were downloaded as position weight matrices and screening was processed on the genome of *E. piscicida* EIB202 by FIMO on MEME Suite ver. 5.5.1. The motif binding score of each position was calculated according to the FIMO output scores and normalized to a range of 0–1.

To validate the in silico predictions, the 6 × His-tagged ArgR was expressed in *E. coli* BL21 with pET28a vector and purified using nickel beads (Sangon Biotech, 20504ES08). The putative promoter region of the test gene for EMSA (−150 to +150 predicted to contain the ArgR binding site) was amplified by PCR. A universal primer sequence (5′-AGCCAGTGGCGA-TAAG-3′) was included in the gene-specific primers and then labeled 5′-biotin with a universal primer. EMSA was performed according to the protocol provided with the chemiluminescent EMSA kit (Beyotime, P0018FS). The purified ArgR was incubated with 0.25 ng biotin-labeled DNA probes in EMSA buffer (10 mM Tris-HCl, 50 mM NaCl, 50 µg/mL poly(d[IC]), 10% glycerol, pH 8.0) at 25 °C for 30 min. The samples were then dissolved in ice-cold 0.5 × Tris-Borate-EDTA at 100 V on a 6.5% non-denaturing PAGE gel. Bands were detected using Omni-ECL™ Pico Light chemiluminescent kit (Epizyme, SQ202L). The plasmid construction and primers used for probe amplification are listed in Supplementary Table S6.

Cell infection

RAW264.7 cells were cultivated in 6-well plates at a density of 1×10^6 cells per well and allowed to adhere overnight. Overnight bacterial cultures were washed three times with PBS and used to infect the cells at a specific MOI of 10 for RAW264.7 cells. After a 2-hour incubation period, the cells were washed twice with PBS and then exposed to a medium containing 1000 µg/ml of gentamicin for 15 min at 35 °C to eliminate extracellular bacteria.

To detect intracellular bacteria, the medium was aspirated and cells were washed twice with sterile PBS. Then, 0.5% Triton X-100 (YEASEN, 20107ES76) cell lysis buffer was added to the cells and incubated for 25 min at 35 °C. Cell lysate samples were collected and serial dilutions were made with sterile PBS followed by the plating on agar plates for CFU enumeration.

To assess bacterial proliferation, after eliminating extracellular bacteria, the medium was replaced with a fresh medium containing 10 µg/ml of gentamicin. The cells were further incubated for an additional 3.5 h at 35 °C. Following a total infection time of 5.5 h, the medium was aspirated and cells were washed twice with sterile PBS. Cell lysis buffer was added to cells followed by incubation for 25 min at 35 °C. Cell lysate samples were collected, serially diluted with sterile PBS, and plated on agar plates for bacterial enumeration. The bacterial numbers obtained from the agar plates were used to calculate CFUs. The CFUs were then converted to cell numbers to determine the bacterial proliferation capacity inside the cells.

To assess gene expression during infection, macrophage-released *E. piscicida* was prepared⁴¹. Briefly, the infected RAW264.7 cells were lysed with 0.5% Triton X-100 at 2 h, 4 h, and 6 h post-infection. The supernatant was separated from cell debris by centrifugation at $600 \times g$ for 5 min. The isolated supernatant was further centrifuged at $12,000 \times g$ for 5 min to collect macrophage-released *E. piscicida*. The collected bacterial pellets were then used for mRNA extraction and gene expression analysis via qRT-PCR.

To measure the changes in intracellular arginine levels during infection, RAW264.7 cells were infected with *E. piscicida* and then lysed with 100 µL of 0.5% Triton X-100. After centrifugation at $600 \times g$ for 5 min, the supernatant was used to determine L-arginine concentration using an ELISA kit (Chenjun, BY-M02120).

In vivo challenge assays in turbot

Healthy turbot weighing 25.0 ± 3.0 g were chosen from a commercial farm in Yantai, China, and maintained in aerated tanks supplied with a continuous flow of seawater at 16 °C. After the acclimation of turbot in the laboratory for 7 days, all *E. piscicida* strains grown in LB medium at 30 °C overnight were harvested by centrifugation at $8000 \times g$ for 2 min and resuspended by sterile PBS three times. The bacteria suspension was quantified to a concentration of 10^8 CFU/ml and was intraperitoneally injected into each turbot at a dose of 10^7 CFU/fish. A total of 15 fish were used for each group and the survival was observed every day for up to 16 dpi to construct a survival curve. On the 10th day post-injection, 3 remaining fish from each group were selected and sacrificed. The harvested liver tissue was homogenized and serially diluted followed by plating on 15 cm DHL agar with four replicates for each tissue sample before incubation at 30 °C overnight.

Statistics and reproducibility

Data were presented as the mean \pm S.D. of triplicate samples per experimental condition unless noted otherwise. Representative results are shown in the figures. Statistical analyses for all bar-plots and box-plots were performed by running unpaired one-tailed Student's *t* test using Microsoft Excel (version 23.11) and the statistical analysis for the results of Fig. 6B was performed using the Log-Rank method from the R package survival (version 3.3.5). differences were considered significant at **P* < 0.05, ***P* < 0.01, and ****P* < 0.001.

Ethics statement

All animal procedures performed were authorized by the animal care committee of the East China University of Science and Technology (2006272). The Experimental Animal Care and Use Guidelines from the Ministry of Science and Technology of China (MOST-2011-02) were rigorously adhered to.

Reporting summary

Further information on research design is available in the Nature Portfolio Reporting Summary linked to this article.

Data availability

The raw data of TIS sequencing analyses were deposited under accession numbers PRJNA1079515. Targeted metabolomics has been deposited in MetaboLights with the identifier MTBLS9590. The mass spectrometry data has been deposited in PRIDE with identifiers PXD047605. A reporting summary for this article is available as Supplementary Information file. The source data underlying Figs. 1–6, Supplementary Fig. 1 and Supplementary Fig. 3 are provided in the Supplementary Data 1. The inhibition zone assay images of the biological replicates underlying Fig. 1D and Fig. 3C can be found in Supplementary Fig. 6. The uncropped and unedited blots can be found in Supplementary Fig. 7. Specific data *P* values are also included within the Supplementary Data 1. Source data are provided with this paper.

Received: 3 July 2024; Accepted: 19 February 2025;

Published online: 28 February 2025

References

- Olzmann, J. A. & Carvalho, P. Dynamics and functions of lipid droplets. *Nat. Rev. Mol. Cell Biol.* **20**, 137–155 (2019).
- Bosch, M. & Pol, A. Eukaryotic lipid droplets: metabolic hubs, and immune first responders. *Trends Endocrinol. Metab.* **33**, 218–229 (2022).
- Hinson, E. R. & Cresswell, P. The antiviral protein, viperin, localizes to lipid droplets via its N-terminal amphipathic alpha-helix. *Proc. Natl. Acad. Sci. USA* **106**, 20452–20457 (2009).
- Anand, P. et al. A novel role for lipid droplets in the organismal antibacterial response. *Elife* **1**, e00003 (2012).
- Bougnères, L. et al. A role for lipid bodies in the cross-presentation of phagocytosed antigens by MHC class I in dendritic cells. *Immunity* **31**, 232–244 (2009).
- Vallochi, A. L., Teixeira, L., Oliveira, K. D. S., Maya-Monteiro, C. M. & Bozza, P. T. Lipid droplet, a key player in host-parasite interactions. *Front. Immunol.* **9**, 1022 (2018).
- Safi, R. et al. Defensive-lipid droplets: Cellular organelles designed for antimicrobial immunity. *Immunol. Rev.* **317**, 113–136 (2023).
- Melo, R. C. & Dvorak, A. M. Lipid body-phagosome interaction in macrophages during infectious diseases: host defense or pathogen survival strategy? *PLoS Pathog.* **8**, e1002729 (2012).
- Knight, M., Braverman, J., Asfaha, K., Gronert, K. & Stanley, S. Lipid droplet formation in *Mycobacterium tuberculosis* infected macrophages requires IFN- γ /HIF-1 α signaling and supports host defense. *PLoS Pathog.* **14**, e1006874 (2018).
- Hüsler, D., Stauffer, P. & Hilbi, H. Tapping lipid droplets: A rich fat diet of intracellular bacterial pathogens. *Mol. Microbiol.* **120**, 194–209 (2023).
- Nawabi, P., Catron, D. M. & Haldar, K. Esterification of cholesterol by a type III secretion effector during intracellular *Salmonella* infection. *Mol. Microbiol.* **68**, 173–185 (2008).
- Kiarely Souza, E. et al. Lipid droplet accumulation occurs early following *Salmonella* infection and contributes to intracellular bacterial survival and replication. *Mol. Microbiol.* **117**, 293–306 (2022).
- Tang, M. et al. *Burkholderia pseudomallei* interferes with host lipid metabolism via NR1D2-mediated PNPLA2/ATGL suppression to block autophagy-dependent inhibition of infection. *Autophagy* **17**, 1918–1933 (2021).
- Bosch, M., Sweet, M. J., Parton, R. G. & Pol, A. Lipid droplets and the host-pathogen dynamic: FATal attraction? *J. Cell Biol.* **220**, e202104005 (2021).
- Bosch, M. et al. Mammalian lipid droplets are innate immune hubs integrating cell metabolism and host defense. *Science* **370**, eaay8085 (2020).
- Doolin, T. et al. Mammalian histones facilitate antimicrobial synergy by disrupting the bacterial proton gradient and chromosome organization. *Nat. Commun.* **11**, 3888 (2020).
- Leung, K. Y., Wang, Q. Y., Yang, Z. & Siame, B. A. *Edwardsiella piscicida*: A versatile emerging pathogen of fish. *Virulence* **10**, 555–567 (2019).
- Aggarwal, P. et al. *Edwardsiella* induces microtubule-severing in host epithelial cells. *Microbiol. Res.* **229**, 126325 (2019).
- Park, S. B., Aoki, T. & Jung, T. S. Pathogenesis of and strategies for preventing *Edwardsiella tarda* infection in fish. *Vet. Res.* **43**, 67 (2012).
- Xie, H. X. et al. *Edwardsiella tarda*-induced cytotoxicity depends on its type III secretion system and flagellin. *Infect. Immun.* **82**, 3436–3445 (2014).
- Wang, X. et al. *Edwardsiella tarda* T6SS component *evpP* is regulated by *esrB* and iron, and plays essential roles in the invasion of fish. *Fish. Shellfish Immunol.* **27**, 469–477 (2009).
- Lu, Y. Z., Zheng, J. Y., Yang, M. J., Wang, Q. Y. & Zhang, Y. X. An *Edwardsiella tarda* mutant lacking UDP-glucose dehydrogenase shows pleiotropic phenotypes, attenuated virulence, and potential as a vaccine candidate. *Vet. Microbiol.* **160**, 506–512 (2012).
- Zhang, R. Y. et al. ArnB mediates CAMP resistance and in vivo colonization in the fish pathogen *Edwardsiella piscicida*. *Aquaculture* **576**, 739855 (2023).
- Daniel, J., Maamar, H., Deb, C., Sirakova, T. D. & Kolattukudy, P. E. *Mycobacterium tuberculosis* uses host triacylglycerol to accumulate lipid droplets and acquires a dormancy-like phenotype in lipid-loaded macrophages. *PLoS Pathog.* **7**, e1002093 (2011).
- Shao, S., Wei, L. F., Xia, F., Zhang, Y. X. & Wang, Q. Y. Defined mutant library sequencing (DML-Seq) for identification of conditional essential genes. *Bio Protoc.* **11**, e3943 (2021).
- Yang, G. H. et al. Time-resolved transposon insertion sequencing reveals genome-wide fitness dynamics during infection. *mBio* **8**, e01581-17 (2017).
- Arena, E. T. et al. The deubiquitinase activity of the *Salmonella* pathogenicity island 2 effector, SseL, prevents accumulation of cellular lipid droplets. *Infect. Immun.* **79**, 4392–4400 (2011).
- Charlier, D. & Bervoets, I. Regulation of arginine biosynthesis, catabolism and transport in *Escherichia coli*. *Amino Acids* **51**, 1103–1127 (2019).
- Chakraborty, B. & Burne, R. A. Effects of arginine on *Streptococcus* mutants growth, virulence gene expression, and stress tolerance. *Appl. Environ. Microbiol.* **83**, e00496–17 (2017).
- Kieboom, J. & Abee, T. Arginine-dependent acid resistance in *Salmonella enterica* serovar Typhimurium. *J. Bacteriol.* **188**, 5650–5653 (2006).
- Qu, D. et al. A new coumarin compound DCH combats methicillin-resistant *Staphylococcus aureus* biofilm by targeting arginine repressor. *Sci. Adv.* **6**, eaay9597 (2020).
- Foster, J. W. & Moreno, M. Inducible acid tolerance mechanisms in enteric bacteria. *Novartis Found. Symp.* **221**, 55–69 (2007).
- Liu, Y. et al. Transcriptomic dissection of the horizontally acquired response regulator *EsrB* reveals its global regulatory roles in the physiological adaptation and activation of T3SS and the cognate effector repertoire in *Edwardsiella piscicida* during infection toward turbot. *Virulence* **8**, 1355–1377 (2017).
- Yin, K. Y. et al. Critical role for a promoter discriminator in RpoS control of virulence in *Edwardsiella piscicida*. *PLoS Pathog.* **14**, e1007272 (2018).
- Fang, Q. et al. TCS regulator *CpxR* of *Edwardsiella piscicida* is vital for envelope integrity by regulating the new target gene *yccA*, stress resistance, and virulence. *Aquaculture* **574**, 739703 (2023).
- Blair, J. M., La Ragione, R. M., Woodward, M. J. & Piddock, L. J. Periplasmic adaptor protein *AcrA* has a distinct role in the antibiotic resistance and virulence of *Salmonella enterica* serovar Typhimurium. *J. Antimicrob. Chemother.* **64**, 965–972 (2009).
- Martí, I., Líndez, A. A. & Reith, W. Arginine-dependent immune responses. *Cell Mol. Life Sci.* **78**, 5303–5324 (2021).

38. Chen, S. et al. Macrophages in immunoregulation and therapeutics. *Sig. Transduct. Tar.* **8**, 207 (2023).
39. Menezes-Garcia, Z., Kumar, A., Zhu, W., Winter, S. E. & Sperandio, V. arginine sensing regulates virulence gene expression and disease progression in enteric pathogens. *Proc. Natl. Acad. Sci. USA* **117**, 12387–12393 (2020).
40. Espinel, I. C., Guerra, P. R. & Jelsbak, L. Multiple roles of putrescine and spermidine in stress resistance and virulence of *Salmonella enterica* serovar Typhimurium. *Micro. Pathog.* **95**, 117–123 (2016).
41. Jiang, J. et al. Bacterial infection reinforces host metabolic flux from arginine to spermine for NLRP3 inflammasome evasion. *Cell Rep.* **34**, 108832 (2021).
42. Miller, J. H. A short course in bacterial genetics: a laboratory manual and handbook for *Escherichia coli* and related bacteria (Cold Spring Harbor Laboratory Press, 1992).
43. Chao, M. C., Abel, S., Davis, B. M. & Waldor, M. K. The design and analysis of transposon insertion sequencing experiments. *Nat. Rev. Microbiol.* **14**, 119–128 (2016).
44. Langmead, B., Trapnell, C., Pop, M. & Salzberg, S. L. Ultrafast and memory-efficient alignment of short DNA sequences to the human genome. *Genome Biol.* **10**, R25 (2009).
45. DeJesus, M. A., Ambadipudi, C., Baker, R., Sassetti, C. & Iøerger, T. R. TRANSIT—A software tool for Himar1 TnSeq analysis. *PLoS Comput. Biol.* **11**, e1004401 (2015).
46. Shao, S. et al. Interplay between ferric uptake regulator Fur and horizontally acquired virulence regulator EsrB coordinates virulence gene expression in *Edwardsiella piscicida*. *Microbiol. Res.* **253**, 126892 (2021).
47. Eckweiler, D., Dudek, C. A., Hartlich, J., Brötje, D. & Jahn, D. PRODORIC2: the bacterial gene regulation database in 2018. *Nucleic Acids Res.* **46**, D320–D326 (2018).
48. Cho, S. et al. The architecture of ArgR-DNA complexes at the genome-scale in *Escherichia coli*. *Nucleic Acids Res.* **43**, 3079–3088 (2015).
- administration: Y.X.Z.; Supervision: Q.Y.W., S.S.; Validation: Q.Y.W., S.S.; Visualization: Y.P., Y.H.L., S.S.; Writing – original draft: Y.P., S.S.; Writing – review and editing: S.S.

Competing interests

The authors declare no competing interests.

Additional information

Supplementary information The online version contains supplementary material available at <https://doi.org/10.1038/s42003-025-07777-7>.

Correspondence and requests for materials should be addressed to Shuai Shao.

Peer review information *Communications Biology* thanks Rémi Safi and the other, anonymous, reviewer(s) for their contribution to the peer review of this work. Primary Handling Editors: Karthika Rajeeve and Tobias Goris. A peer review file is available.

Reprints and permissions information is available at <http://www.nature.com/reprints>

Publisher's note Springer Nature remains neutral with regard to jurisdictional claims in published maps and institutional affiliations.

Open Access This article is licensed under a Creative Commons Attribution-NonCommercial-NoDerivatives 4.0 International License, which permits any non-commercial use, sharing, distribution and reproduction in any medium or format, as long as you give appropriate credit to the original author(s) and the source, provide a link to the Creative Commons licence, and indicate if you modified the licensed material. You do not have permission under this licence to share adapted material derived from this article or parts of it. The images or other third party material in this article are included in the article's Creative Commons licence, unless indicated otherwise in a credit line to the material. If material is not included in the article's Creative Commons licence and your intended use is not permitted by statutory regulation or exceeds the permitted use, you will need to obtain permission directly from the copyright holder. To view a copy of this licence, visit <http://creativecommons.org/licenses/by-nc-nd/4.0/>.

© The Author(s) 2025

Acknowledgements

The authors thank Dr. Yu-Feng Yao (Shanghai Jiao Tong University School of Medicine) for sharing *E. coli* O157:H7 EDL933. This work was supported by grants from the National Natural Science Foundation of China (32130108, 32373183) and the China Agriculture Research System of MOF and MARA (CARS-47).

Author contributions

Conceptualization: Q.Y.W., S.S.; Data curation: Y.P., S.S.; Funding acquisition: Q.Y.W.; Investigation: Y.P., Y.H.L., J.Z.W.; Project